HHS Public Access

Author manuscript

Exp Cell Res. Author manuscript; available in PMC 2020 August 01.

Published in final edited form as:

Exp Cell Res. 2019 August 01; 381(1): 18–28. doi:10.1016/j.yexcr.2019.05.005.

Quantitative assessment of changes in cell growth, size and morphology during telomere-initiated cellular senescence in *Saccharomyces cerevisiae*

Neda Z. Ghanem, **Shubha R. L. Malla**, **Naoko Araki**, and **L. Kevin Lewis***

Department of Chemistry and Biochemistry, Texas State University, San Marcos, TX 78666

Abstract

Telomerase-deficient cells of the budding yeast *S. cerevisiae* experience progressive telomere shortening and undergo senescence in a manner similar to that seen in cultured human fibroblasts. The cells exhibit a DNA damage checkpoint-like stress response, undergo changes in size and morphology, and eventually stop dividing. In this study, a new assay is described that allowed quantitation of senescence in telomerase-deficient *est2* cells with applied statistics. Use of the new technique revealed that senescence was strongly accelerated in *est2* mutants that had homologous recombination genes *RAD51*, *RAD52* or *RAD54* co-inactivated, but was only modestly affected when *RAD55*, *RAD57* or *RAD59* were knocked out. Additionally, a new approach for calculating population doublings indicated that loss of growth capacity occurred after approximately 64 generations in *est2* cells but only 42 generations in *est2 rad52* cells. Phase contrast microscopy experiments demonstrated that senescing *est2* cells became enlarged in a time-dependent manner, ultimately exhibiting a 60% increase in cell size. Progressive alterations in physical properties were also observed, including striking changes in light scattering characteristics and cellular sedimentation rates. The results described herein will facilitate future studies of genetic and environmental factors that affect telomere shortening- associated cell senescence rates using the yeast model system.

Keywords

telomerase; senescence; aging; homologous recombination; checkpoint

1. Introduction

Telomerase is an RNA-dependent DNA polymerase complex that replicates the ends of chromosomes at regions called telomeres in most eukaryotes. It has reverse transcriptase

*Corresponding author: L. Kevin Lewis, Chemistry and Biochemistry, Texas State University, 601 University Drive, San Marcos, TX 78666 LL18@txstate.edu, Phone: 512-245-8594, Fax: 512-245-2374.

Declaration of conflict of interest

None.

activity that adds short telomeric repeat sequences to the 3' ends of chromosomal DNA during S phase of the cell cycle [1–5]. The enzyme is critical because it allows cells to overcome the end replication problem, which arises because the major DNA polymerases in the cell cannot completely replicate the ends of linear chromosomes [6–8].

Absence of telomerase results in progressive shortening of telomeres in dividing cells *in vitro* and also *in vivo*. Most human cells reduce production of telomerase during embryonic development, leading to shortening of telomeres as humans age. Humans of the same age can have different average telomere lengths and older individuals with the shortest telomeres are at higher risk of developing several age-related diseases [1,8]. Several studies have provided evidence that telomere lengths monitored within blood cells can be affected positively or negatively by lifestyle choices, including activities related to smoking, stress, exercise, and food intake [1,9–14]. Although most human somatic cells do not produce telomerase, approximately 90% of cancer cells have reactivated telomerase expression, which results in immortalization of the cells. This observation has stimulated research into the development of new anti-cancer therapies that target telomerase and/or telomeres to limit the lifespans of cancer cells [15–19].

Primary human fibroblast cells propagated in liquid cell culture mimic the telomere shortening observed *in vivo*, undergoing approximately 25–40 population doublings before the cells stop dividing. This phenomenon is called telomere-initiated cellular senescence or *in vitro* cell aging and is due to progressive telomere shortening in the cells caused by absence of telomerase. Many alterations occur in the cells during the advancement of senescence, including accumulation of modifications in nuclear DNA, changes in expression and secretion of different proteins, alteration of cell morphology and cell surface antigens, and activation of cellular stress responses [20–27]. An important concept that has emerged in recent years is that humans and animals may accumulate dysfunctional cells with the characteristics of cultured senescent cells in tissues and organs during normal aging and that these senescent-like cells might become targets of anti-aging therapy [22,24,25,28–34].

Saccharomyces cerevisiae, a unicellular eukaryote referred to as budding yeast, has proven to be an important experimental model to study the senescence process, in large part because of the sophisticated molecular genetics techniques available for investigation of this organism [35–40]. The composition of yeast telomerase is analogous to the telomerase complex of humans, consisting of multiple protein subunits plus an RNA component that serves as template for new DNA synthesis [39–41]. The core yeast telomerase enzyme consists of the Est1, Est2, and Est3 proteins along with *TLC1* RNA. Est2 is the catalytic component and is functionally equivalent to hTERT, the reverse transcriptase subunit of human telomerase.

Inactivation of the yeast *EST1, EST2, EST3* or *TLC1* genes causes progressive telomere shortening and cellular senescence (loss of growth capability) after approximately 60–70 cell cycles, a process that is similar to that seen in primary human cells propagated in liquid culture. Yeast cells undergoing senescence become larger in size and accumulate increasing numbers of G_2 phase cells while undergoing a DNA damage-induced cell cycle checkpoint arrest response that requires some, but not all, of the checkpoint genes associated with a

conventional DNA damage response [42–44]. Telomerase reactivation and mating rescue experiments demonstrated that most non-dividing, fully senescent yeast cells do not lose viability, but instead exist in a metabolically active, growth-arrested state [42]. Telomere shortening rates vary among different cells and therefore *in vitro* cell aging is a stochastic process, whereby individual cells lose their capacity for additional growth at different times. The senescence process has been monitored in telomerase-deficient yeast cells using both solid media plate assays and liquid culture assays [35,37–40,42,45,46]. Plate assays involve streaking cells from single colonies onto the surfaces of fresh plates, allowing the cells to grow into new colonies, and then streaking the cells out again and again from individual colonies until there is a strong reduction in the numbers and the sizes of new colonies that form. Typically, this takes three or four streak plates and a total of approximately 60–70 cell divisions [35,39,42].

The major goal of the current study was to develop new methods to analyze the kinetics of cellular senescence and to quantify the changes that occur in the morphology and physical properties of the cells. A new plate-based senescence assay is described that allowed cell aging rates to be monitored quantitatively and permitted application of several commonly used statistical measures. In addition, a cell division counting method was developed to calculate the number of generations of growth achieved by the cells. The plate assay and the cell division counting system were subsequently used to quantify the strong acceleration of senescence that occurs in telomerase-deficient cells that are also defective in genes affecting homologous recombination. Other changes occurring in senescing cells were also analyzed, including time- dependent increases in the sizes of the cells, which could be correlated with changes occurring in the physical properties of the cells.

2. Materials and Methods

2.1. Yeast strains and plasmids

All yeast strains used for this project were derived from BY4742 (*MATα his3Δ1 leu2 Δ0 lys2Δ0 ura3Δ0*) [47]. These strains included YLKL803 (BY4742, *est2Δ::HygB*^{r} containing pLKL82Y [*CEN/ARS URA3 GAL1-V10p::EST2*]) and YLKL807 (*est2Δ::HygB*^{r} *rad52Δ::G418*^{r} + pLKL82Y), which have been described [42,48]. YLKL961 (*est2Δ::HygB*^{r}) is derived from YLKL803 but contains pVL715 [*2μ URA3 ADH1p::EST2*]) [49] rather than pLKL82Y. Double mutant derivatives of YLKL803 were created by either plasmid or PCR fragment-mediated gene disruption-deletion as described [50]. These strains included YLKL1203 (*est2Δ::HygB*^{r} *rad51Δ:LEU2*), YLKL1204 (*est2Δ::HygB*^{r} *rad54Δ:LEU2*), YLKL1205 (*est2Δ::HygB*^{r} *rad57Δ:LEU2*), YLKL1534 (*est2Δ::HygB*^{r} *rad55Δ:LEU2*), and YLKL1547 (*est2Δ::HygB*^{r} *rad59Δ:LEU2*).

2.2. Yeast cell growth and transformation

Yeast growth media, including YPDA, YPG and synthetic dropout media, were prepared as described [51]. Transformation of DNA into yeast cells was performed using early stationary phase cells and a PEG/LiAc chemical-based method [52]. Synthetic media plates containing 2% glucose and 1% 5-fluoroorotic acid (5-FOA) (Gold Biotechnology) were used for counterselective growth of Ura$^-$ cells. Plasmid DNAs were extracted from *E. coli* DH5a

cells grown in liquid TB broth using Qiaprep plasmid miniprep kits. Horizon 11–14 gel rigs were used to perform gel electrophoresis using 0.7% - 0.9% agarose gels in 1 X TAE buffer (40 mM Tris, 20 mM acetic acid, 1 mM EDTA). Gels were stained in ethidium bromide (0.5 μg/mL) for 15–20 min and images were captured using an Alpha Innotech Red Imaging system.

2.3. Solid media-based senescence assays

New senescence assays involving telomerase-deficient YLKL803 cells employed either rich YPDA or synthetic (defined) plate media and were accomplished by performing a series of streaks using toothpicks. For the first streak, cells were picked from a freshly grown galactose minus uracil stock plate so that cells were producing telomerase from the *GAL1-V10p::EST2* plasmid pLKL82Y prior to initiation of the experiment. Cells from a single colony were touched with a toothpick and streaked onto new plates as double columns (shown in Figure 2A). After the first rectangular column was created by repeatedly making overlapping parallel lines with a sterile toothpick, the toothpick was flipped and used to pull cells from the bottom of the first column over to where the second column was to be initiated. A new toothpick was then used to streak a complete second column (rectangle). The second column was always streaked away from the center so that individual colonies formed closer to the outer edges of the plate.

For each plate, four separate double columns were streaked so that single colonies became visible after incubation of the plates for 3–4 days at 30°C (see plate photographs in Figure 2A and 2C). For the second streak, small-to-medium sized (typically 0.8 – 0.9 mm diameter) single colonies from the first streak plate were picked and streaked into new double columns onto new plates. This process was performed again to streak cells from the second plate to the third streak plate. Altogether, four separate double columns were streaked per plate and cells were allowed to grow in the incubator at 30°C for 3–4 days, depending on the growth rate of the colonies. Slow- growing double mutants were sometimes grown for an extra day to ensure that the sizes of the picked colonies were similar for all strains. For the fourth streak, 48 different individual colonies were picked and streaked as single tall rectangular columns onto 6 different plates using a grid pattern placed underneath the plates, creating 8 separate columns on each plate as shown in Figure 2. These plates were incubated at 30°C for 4 days. As cells aged, their growth rates slowed, which is why the last streak plates were always incubated for 4 days. Full columns were defined as complete rectangles with confluent growth throughout, i.e., without internal gaps and without shortening of growth on one end. Examples are presented in Figure 2A. Data from the plate assays were analyzed and mean, median, standard deviation and unpaired Student’s T-test results calculated as appropriate. Results obtained with the new grid-based assay were highly reproducible, as shown by the multiple trials presented in the text and also the similar results that have been observed by students working in the lab over the past 5 years.

2.4. Determination of the number of cell divisions completed during senescence on plate media

The method used for calculation of the number of generations of growth within colonies was conceptually similar to the approach used by Joseph and Hall [53], but details had to be

worked out empirically to ensure that all cells within the colonies were harvested and counted. Initial experiments established that the bore sizes of conventional glass Pasteur pipettes were not large enough to core entire colonies reliably. Testing of several alternatives led to the determination that a 1 mL graduated plastic pipette with an attached electronic pipette aid could be used to core all cells from typical small-to-medium sized colonies. The electronic pipette aid was used to pull the colony, along with the plate agar beneath it, up into the 1 mL pipette (photos explaining the process are presented in Figure 4A). After expulsion of the plug of agar containing the colony into water, tests demonstrated that it was important to rinse the plastic pipette 3–4 times with water from the recipient microfuge tube, which contained either 500 μL or 1000 μL of sterile deionized water. The tube was mixed using a vortexer adjusted to its highest setting for 10 s to separate the cells from the agar and then sonicated for 10 s at amplitude 24 with a Sonics and Materials VCX130 sonicator. A total of 12 μL of cells were transferred onto a hemocytometer and analyzed using a United Scope Model M837T video camera-linked phase contrast microscope to determine cell density. For each assay, 7 to 10 colonies were harvested and used to calculate averages and standard deviations. The average number of cells per colony was used to calculate how many cell divisions were completed by the cells on each streak plate. Defining the variable y as the number of doublings undergone by a single cell to form a colony, the total number of cells in a colony was calculated as 2^y (e.g., after one cell divides twice it will form 4 cells and this can be represented as $2^2 = 4$ total cells; other examples are shown in Figure 4B). Similarly, if 6 cells are present, then 2.5 generations of growth have occurred, corresponding to two complete doublings plus half of a third doubling.

2.5. Measurement of senescent cell sizes

Cells from each senescence assay streak plate were diluted into dH_2O, sonicated 15 s and analyzed by phase contrast microscopy. The image capture program ScopeImage DynamicPro was used to visualize fields of cells at 400×-1000× with a length scale overlaid on each field as shown in Figure 5B. The largest diameter of each unbudded cell and the maximum diameter of the mother cell within each budded cell was determined. A total of 10 to 15 cells were measured for each stage of senescence and the results were averaged.

2.6. Analysis of light scattering and cell sedimentation rates

Cells from each senescence streak were harvested from a YPDA plate, rinsed with dH_2O, sonicated, counted by hemacytometer, and diluted to 1×10^7 cells/mL in 0.5 mL dH_2O. Solutions were placed into standard minicuvettes, mixed, and light scattering immediately assessed at 600 nm. Five replicates were analyzed for each sample. Cells were also analyzed at 1×10^6 cells/mL (not shown), which produced OD_{600} values of 0.12 and 0.15 for WT and senescent cells, respectively.

For sedimentation rate tests, cells were sonicated and counted as before and diluted to 1×10^7 cells/mL in 2 mL dH_2O. The cells were then re-sonicated for 15 s, followed by aliquotting of 450 μL into four standard minicuvettes (height: 4.5 cm). After mixing briefly by pipetting up and down in all cuvettes, an initial OD_{600} was measured that corresponded to T=0. Subsequently, OD_{600} values were recorded at 10 min intervals for 70 min using a Bio-Rad Smartspec Plus spectrophotometer. All initial OD_{600} readings were between 1.0

and 1.5. Four replicates were analyzed for each strain and averages and standard deviations are presented in each graph.

3. Results

3.1. Development of a new assay for measuring senescence kinetics

Wildtype yeast cells are routinely grown on Petri dishes, where they form colonies that can be picked with a sterile toothpick or loop and restreaked to form new colonies essentially indefinitely. By contrast, telomerase-deficient cells, i.e., *est1*, *est2*, *est3* or *tlc1* mutants, undergo progressive telomere shortening and can be restreaked only a limited number of times before the cells cease dividing. This form of *in vitro* cell aging is a stochastic process and therefore the number of cell cycles that each cell can complete before losing the capacity to continue dividing is variable. Because of this variability, it has proven difficult to perform quantitative comparisons of senescence kinetics among different mutants or under different environmental conditions using plate assays.

We have previously described a yeast strain (YLKL803) that has been engineered to allow expression of Est2, the catalytic subunit of telomerase, to be modulated using the galactose-inducible *GAL1-V10* promoter [42,48] (Figure 1A). The cells produce Est2 and grow normally when propagated on media containing galactose as carbon source, but upon transfer to glucose media the cells undergo telomere shortening and subsequent senescence. Thus, the cells grown in glucose can be picked from colonies and re-streaked to new plates only a limited number of times. A typical senescence assay is shown in Figure 1B, in which cells were initially picked from a single colony on a synthetic galactose plate lacking uracil and streaked to a glucose-containing YPDA plate, shown as the 1st streak in the figure. New colonies formed after incubation of the plates for 3 days at 30°C. A single colony from the 1st streak plate was then picked and streaked to a 2nd plate and the process was repeated two more times. The cells readily grew into small-to-medium sized colonies on the first three streak plates but show reduced colony-forming ability on the 4th streak. Although the progression depicted on the left side of Figure 1B is similar to those that are commonly reported, the numbers and the sizes of colonies observed on 4th streak plates are variable in practice; several additional 4th streak outcomes are shown on the right side of the figure to illustrate typical variations.

After testing several potential improvements, a new single column growth assay was developed in order to make the senescence assay more quantifiable. In the standard version of the new assay, cells are restreaked from colonies as shown in Figure 1B for the first three streak plates. However, for the 4th plate, individual colonies from the 3rd streak plate are picked and streaked as equal-sized rectangular columns using a grid placed under the plate as a guide (Figure 2A). The plates are then incubated at 30°C for 3 or 4 days. In a typical experiment, streaks 1, 2 and 3 are performed eight times on two plates each, picking from a separate colony for each new streak (Figure 2B). Then, for the 4th streak, 48 single colonies from the 3rd streak plates are streaked into rectangular columns on six new plates using the grids, creating eight columns per plate. The number of columns showing confluent growth are then scored. Examples of full columns formed by wildtype cells are shown in Figure 2A (right side) and examples of each step in the assay for the *est2* strain YLKL803 are shown in

Figure 2C. An important advantage of this approach is that the 4th streak plates essentially represent 48 separate scorable assays of growth capability and this large number allows for the application of statistics.

To investigate the reproducibility of this approach to quantitation of senescence, three separate assays were performed weeks apart from each other by streaking YLKL803 cells from galactose minus uracil plates, ensuring that cells were Est^+ initially, onto YPDA glucose plates (rich growth media). Three additional assays were performed by streaking cells from the galactose minus uracil plates to less nutrient-rich synthetic glucose complete plates, which is the other major type of growth media used in yeast research laboratories (Figure 3A). A control experiment was performed by streaking the cells repeatedly to galactose minus uracil (Gal-Ura) plates, keeping *EST2* expression on throughout the assay. As expected, almost all cells that were grown continuously on galactose plates were able to form full columns on the 4th streak plates (46 out of 48) and there was an average of 7.6 full columns out of 8 total columns on each plate. By contrast, YLKL803 cells propagated on YPDA plates only formed 1.8, 2.0 and 1.8 full columns per 4th streak plate (Figure 3A). Similarly, cells repeatedly streaked to synthetic glucose plates formed only 3.3, 3.0 and 3.5 confluent columns per plate on the 4th streak. Application of the Student's T-test indicated that the results of each glucose assay were strongly different from the control galactose assay ($p < .005$). However, comparing the trials on different media to each other (YPDA-trial 1 vs synthetic glucose complete-trial 1, etc.) yielded p values of 0.31, 0.36 and 0.15 for trials 1, 2 and 3, indicating that the differences seen on rich versus synthetic plates were not significant. Median values were close to the corresponding means, suggesting minimal skewing of the distribution of values in each assay. The standard deviation calculated for the control galactose assay was low (< 10% of the mean), but was high relative to each mean for the senescent cells (Figure 3A), which is a consequence of the stochastic nature of the process. Overall, these findings are an indication that the senescence occurring in the cells could be quantified with good reproducibility.

As shown in Figures 1B and 2C, growth of colonies is typically robust on the third streak plate, after which the cells have undergone approximately 60 generations of growth (assuming approximately 20 cell divisions are required to form a small-to-medium sized colony on a plate; this assumption is addressed more fully below). To determine if senescence might be detectable on the 3rd streak plate, new experiments were performed in which cells were streaked for colonies on plates 1 and 2 but were streaked into scorable columns using grids on the 3rd plate. Two trials using YLKL803 produced 42 and 47 full columns out of 48 total (Figure 3B). The strong growth suggests that senescence is not yet measurable at this stage of the process in the *est2* single mutants.

3.2. Analysis of cell senescence in telomerase-deficient cells that are also defective in homologous recombination

It is well established that *est2 rad52* double mutants, which are telomerase-deficient and also strongly defective in homologous recombination, undergo loss of growth potential earlier than *est2* single mutants, primarily due to faster telomere shortening in cells that cannot restore telomere lengths by unequal strand exchange [39,40,42,46,54]. In conventional plate

senescence assays this characteristic of *est2 rad52* cells manifests as a qualitative reduction in colony numbers and sizes on the 3rd streak plate rather than the 4th plate, but with variability in growth on this streak plate as described above. New assays were performed using *est2 rad52* double mutants (YLKL807), whereby cells were streaked for colonies normally on plates 1 and 2 but were streaked into scorable single columns using grids on the 3rd plate. Colonies were always allowed to grow to the same approximate size on the first and second streak plates, which required an extra day of growth for the slower growing *est2 rad52* double mutants. The recombination-deficient mutant cells produced only 6 and 7 full columns among 48 total column assays (Figure 3C), a strong reduction compared to the 42–47 columns seen with *est2* single mutants (Figure 3B). Analysis of the double mutant strain data using unpaired Student's t-tests to compare trial 1 and trial 2 in Figures 3B and 3C revealed strong differences with $p < 0.005$.

In addition to Rad52, several other members of the RAD52 epistasis group of homologous recombination proteins are also involved in genetic exchange between chromosomes [55–57]. New tests were performed to assess the impacts of other members of this group on senescence. Growth of *est2*, *est2 rad51*, *est2 rad52*, *est2 rad54*, *est2 rad55*, *est2 rad57* and *est2 rad59* strains was analyzed using 3rd streak plates as for Figures 3B and 3C and results are presented in Figure 3D. Inactivation of *RAD51*, *RAD52* and *RAD54* had the greatest impact on senescence, as these mutants generated only 1.2, 0.7 and 1.0 full columns per 3rd streak plate versus 7.5 full columns for *est2* single mutants. Growth of all of the recombination mutants was reduced relative to *est2* cells with $p < 0.05$, though the results with *est2 rad59* cells barely achieved significance at $p = 0.03$ (Figure 3D).

3.3. The new assay produces similar results using an alternative yeast assay strain

The new assay was further assessed using a different senescence strain system. An *est2* strain was constructed (YLKL961) that contains the plasmid pVL715 (*ADH1p::EST2 URA3*) and therefore constitutively produces Est2 protein from the *ADH1* promoter. This strain was maintained on glucose plates lacking uracil so that all cells were $Est2^+$ prior to the assay. The cells were then streaked onto synthetic glucose plates containing 5-FOA (streak #1) using the pattern shown in Figure 2C to select for cells that had spontaneously lost the plasmid and therefore become $Est2^-$. Colonies on the 5-FOA plates were subsequently picked and streaked for single colonies two more times (streak plates 2 and 3) onto glucose complete plates and then into grid-based columns on the 4th streak plates. The average number of full columns formed after growth for 4 days at 30°C on the 4th streak was 3.3 out of 8 total on each plate (Figure 3E). This result is similar to the values of 3.3, 3.0 and 3.5 measured with the original assay system that also used synthetic glucose plates (Figure 3A, Glu-complete media).

3.4. Calculation of population doublings occurring during senescence

The goal of the next experiment was to develop a method to quantify the number of generations (i.e., cell divisions or population doublings) undergone by the senescing cells before they stopped dividing. This was accomplished by harvesting whole YLKL803 strain colonies from streak plates 1, 2 and 3, counting the total number of cells per colony, and then calculating how many generations of growth from a single cell led to that number of

total cells. The final method that was devised involved coring each colony using a long 1 mL pipette connected to an electronic pipette controller, transfer of the cells into water followed by vortexing and sonicating, and counting by hemacytometer in a phase contrast microscope (see caveats and details in Materials and Methods). The steps of the procedure are depicted in Figure 4A. The number of generations achieved was calculated from the total number of cells in each colony. After being streaked to a plate surface, each individual cell divides into 2 cells and then 4 and 8 and so on multiple times to form a single colony of more than a million cells (Figure 4B). The total number of cells present in a single colony can be calculated by using the formula: 2^y = total number of cells. The variable y is the number of cell divisions that have occurred during formation of the colony. As an example, Figure 4B shows that a colony that has 1,048,576 cells has undergone exactly 20 cell divisions. A caveat to this type of analysis is that there may be some cells in the colony that have lost viability and so these numbers should be considered best estimates. YLKL803 colonies formed on rich YPDA plates and on synthetic glucose plates were analyzed in this manner and results are shown in Figures 4C and 4D. The senescing cells underwent a total of 64.7 and 63.3 generations of growth on YPDA and synthetic plates, respectively. Note that these numbers do not take into account the small, variable number of cell divisions that may occur on the subsequent 4th streak plates. We have previously demonstrated that cells harvested from 3rd streak plates exhibit a low average plating efficiency of 0.5%, i.e. only about 1 in 200 cells are able to form colonies when spread onto YPDA plates [42].

In contrast to the *est2* single mutants, *est2 rad52* double mutants completed only 42.3 and 42.7 generations on YPDA and synthetic glucose plates before undergoing loss of growth capability (Figure 4E and 4F). These findings and those resulting from the earlier column assays are important because they show that a difference between yeast strains that has previously been characterized qualitatively using plate media can be analyzed in a more quantitative manner.

3.5. Cell sizes increase progressively during senescence

Senescence leads to changes in size and morphology among aging yeast cells and also in cells of higher eukaryotes [39,43,44]. An example of this phenomenon is depicted in Figure 5A, where the senescent cell population is seen to have larger cells and also more large-budded cells. A phase contrast microscope equipped with a length scale (Figure 5B) was used to measure the average diameters of wildtype cells and *est2* cells harvested at different stages of the senescence process. The cells were taken from YPDA streak plates 1, 2, 3 and 4 (with streaks performed as in Figure 2C), which corresponded to approximately 21, 42, 63 and >63 generations of growth (numbers taken from Figure 4C). Because unbudded G_1 cells tend to be smaller than budded S and G_2/M cells, these two types of cells were measured separately. The maximum diameter of the slightly oval unbudded cells was determined and the largest diameter of the mother cell was assessed in budded cells. A progressive increase in cell size was observed for both cell types (Figure 5C and 5D). Unbudded cell sizes increased from 5.2 μm to 8.2 μm, a 58% gain, and budded cell diameters progressed from 6.3 μm to 10.1 μm, a 60% increase, by the 4th streak. A similar trend was observed in *est2 rad52* double mutants, i.e., unbudded and budded cells got progressively larger during the course of senescence (Figure 5E and 5F). The magnitude of the increase was reduced in the

double mutants, possibly because the *est2 rad52* cells were larger than normal before senescence began, e.g., sizes of the non-senescent double mutants were 7.5 and 8.3 mm while the *est2* single mutants were only 5.2 and 5.7 μm (compare first columns of Figure 5E and 5F vs. first columns of 5C and 5D).

3.6. Senescence also produces changes in the physical properties of the cells

The large alterations in morphology seen in senescent *est2* cells suggested that there might also be measureable changes in the physical properties of the cells, a phenomenon that has not been explored previously. To test this idea, the ability of the cells to scatter visible light (a characteristic of particles suspended in aqueous solutions) and to settle quickly to the bottom of tall cuvettes was examined. Wildtype and senescent cells taken from 4th streak YPDA plates were sonicated, counted by hemacytometer, diluted to 1×10^7/mL, and their ability to scatter light at 600 nm was assessed. The senescent cells exhibited a 33% increase in light scattering (Figure 6A).

Yeast cells, like other eukaryotic cells, will slowly settle to the bottom of aqueous solutions over time. We hypothesized that the larger sizes of senescent cells would cause them to sediment faster than wildtype cells and that this phenomenon could be quantified spectrophotometrically by monitoring the time-dependent decrease in OD_{600} of cell suspensions (illustrated in Figure 6B). Both wildtype and senescent cells propagated on rich YPDA media were harvested, washed, counted and suspended in water at 1×10^7 cells per mL. Sonicated cell aliquots were placed into four cuvettes, mixed, and then OD_{600} values were recorded at 10 min intervals. The senescent cells fell out of solution more quickly than wildtype cells (Figure 6C). The OD_{600} of senescent cells grown on YPDA plates was reduced to 50% after 20 min, while a similar decrease in WT cells required 50 min. Analysis of senescing cells harvested from 1st, 2nd, 3rd, and 4th streak YPDA plates revealed a continuous increase in sedimentation rates for cells taken from each of the first 3 streak plates, though with only a small change from the 3rd to the 4th streak (Figure 6D). Qualitatively similar results were observed when cells were propagated on synthetic glucose complete plates, where the OD_{600} of the senescent cells was decreased by 50% within 25 min, but a similar reduction in WT cells required 38 min (Figure 6E and 6F). Analysis of sedimentation of *est2 rad52* double mutants grown on YPDA media revealed a different, more compressed pattern than *est2* single mutants grown on YPDA plates (compare Figure 6G vs. 6D). This is likely due to the smaller differences in size between senescent and non-senescent *est2 rad52* double mutants described above. In aggregate, these spectrophotometry results demonstrate additional, previously uncharacterized properties of senescent *est2* cells that are strikingly different from wildtype cells.

4. Discussion

Yeast cells have proven to be an important and versatile model system for analyzing genetic factors that affect *in vitro* cell aging. In the current study we have improved the usefulness of this model by developing and testing new assays that allow quantitation of several of the progressive changes that occur in the cells during senescence. Telomerase-deficient cells lose telomere sequences during each cell cycle and cease growing after some number of

their telomeres reach critically short lengths, but the precise number of cell divisions required to reach this state varies. This stochastic nature of senescence has made it difficult to quantify the process using plate assays. The single column assay method described here was found to give reproducible results in multiple trials when employed using either YPDA plates or synthetic glucose plates. In addition, similar results were observed with a strain that modulated telomerase expression using a *GAL1-V10p::EST2* cassette and a different strain in which a *URA3* plasmid containing a constitutive *ADH1p::EST2* promoter fusion was removed by selection on 5-FOA plates.

Lundblad *et al.* have previously described another approach to analyzing senescence using plate assays that, like the one described here, attempted to reduce the subjectivity of the analysis [35,58,59]. In that method, telomerase-deficient cells were streaked from single colonies onto new plates a total of three times, streaking/diluting the cells each time so that new colonies formed on the streaked plates. The amount of colony growth visible on each plate was then analyzed in a genotype-blind manner, whereby the viewer did not know what specific strain was being analyzed, and growth extent was then classified into one of either 5 or 6 different categories ranging from approximately no growth to nearly wildtype levels of growth. Both this earlier approach and the system developed and tested in the current study are superior to other plate-based assays because of their use of many replicates for the analysis and their ability to generate numerical growth scores for different strains. A potential advantage of the full column scoring method described here is that it reduces subjectivity even further, i.e., one simply determines whether or not the cells streaked from an individual colony grew into a confluent full column.

A major advantage of the new plate assay is its ability to compare senescence progression in mutant strains with altered telomere shortening rates. For example, it has been known for many years that reduction of homologous recombination between telomeres accelerates cellular senescence [35,39,42,45,46]. Using the new method, the faster kinetics of senescence in homologous recombination-deficient *est2 rad52* cells could be readily expressed in numbers, i.e., *est2* cells formed 42 columns out of 48 tested under conditions where *est2 rad52* double mutants generated only 6 full columns (Figure 3B and 3C, trial 1). A more critical assessment of this approach was performed by analyzing senescence in a series of isogenic telomerase-deficient cells that also contained mutations in several other RAD52 group genes. The experiments demonstrated that senescence was accelerated in all of the recombination-deficient mutants and that inactivation of *RAD51*, *RAD52* and *RAD54* had the most severe impacts. This result is in accord with past studies showing that ionizing radiation resistance and some types of recombination events are more strongly reduced in *rad51*, *rad52* and *rad54* mutants than in *rad55*, *rad57* and *rad59* cells [55,56,60,61–65]. The results are also largely consistent with those of a prior study that used liquid culture-based senescence assays to analyze growth of *tlc1* strains lacking Rad51, Rad52, Rad54 or Rad57 [66]. In that work, growth in liquid broth was strongly reduced in all four recombination-deficient double mutants, with *tlc1 rad52* and *tlc1 rad54* cells showing the largest effects.

The number of cell cycles completed by senescing cells was guaged using a colony harvesting technique developed for this study (Figure 4A). The method allowed determination of the number of generations of growth completed by *est2* versus *est2 rad52*

cells prior to the last streak plate, on which colony growth is poor and variable. The analysis showed that *est2* cells completed 64.7 cycles in YPDA plate assays under conditions where *est2 rad52* cells completed only 42.3 cycles. This analysis of the number of population doublings represents a second approach, in addition to the plate assays described above, that was used to measure the accelerated senescence of telomerase-deficient *rad52* mutants quantitatively.

Several past studies have analyzed yeast cell senescence using liquid culture assays, a method that can potentially also be employed to calculate the number of generations of growth achieved during senescence [39,42–45]. In this method, cells are diluted to a low cell titer in liquid broth and then shaken overnight. The dense cell cultures formed on the following day are diluted to a low titer into fresh broth and shaken overnight again and the process is repeated for several days until a strong reduction in growth is observed. The density of each overnight culture decreases due to senescence over the course of several days, and then begins to go back up again as individual cultures accumulate faster-growing survivor mutants that utilize an alternative, telomerase-independent mechanism for maintaining telomere lengths [37,39,40,67]. In practice, the number of generations and/or days that occur before the cell titer of the overnight culture reaches a minimum density and begins to increase due to accumulation of survivor mutants shows strong variability. Examples of this variability among independent cultures analyzed in a single study can be found in the reports by Ijpma and Greider, Azam *et al.* and Chang *et al.* [44,45,68]. The generations of growth completed before reaching a minimum in telomerase- deficient *tlc1* cells (equivalent to the *est2* mutants studied here) ranged from approximately 60 to 85. Thus, the results of liquid-based assays that reported generation numbers are in general agreement with those obtained in the current study. Although survivor mutants accumulate and eventually take over liquid cultures of telomerase-deficient cells, the plate senescence assays are largely unaffected by this process. Large colonies that may contain fast-growing survivor mutant cells are occasionally observed within 4th streak plate columns, but their appearance is rare and does not interfere with analysis of growth within the 48 individual assays.

Yeast cells become larger than normal during the senescence process [43,44,69]. We calculated maximum cell diameters at each stage of the plate senescence process and observed a time-dependent increase in size. The increases were found to be substantial, as final average sizes were elevated by 60% among both unbudded and budded cells. Consistent with these findings, there were strong changes in the physical properties of the cells. Using simple spectrophotometric assays, we observed that senescent cells induced light scattering more strongly than normal cells. The ability of eukaryotic cells to scatter light has been demonstrated to be dependent on multiple factors [70–72], but it is likely that the greater overall sizes and the elevated fraction of large-budded (dumbbell-shaped) cells among the senescent cells are major contributors. We also observed that the older cells sedimented out of solution at a faster rate than wildtype cells and that this rate increased substantially as the cells progressed from early to late senescence. The faster sedimentation effect was strongest in cells that had been propagated on rich YPDA plates, where the time course suggested that 90% of senescent cells had fallen to the bottom of the tubes after 30 min, while only 10% of wildtype cells had sedimented at that time (Figure 6C). It is likely

that this phenotype is also a result of the increased cell sizes and the larger number of large-budded G_2 cells present in senescent cell populations caused by activation of the telomere shortening-associated DNA damage checkpoint response [39,42–44]. The changes in cellular metabolism and the loss of growth capability that occur in cells undergoing telomere shortening have been linked to changes occurring in the chromosomes. However, cells that have become enlarged, regardless of the underlying cause of the enlargement, display defects in cell cycling that are in part to dilution of cytoplasmic components [73]. It is therefore possible that progressive cell enlargement also contributes to the gradual loss of growth capability observed in telomerase-deficient cells.

In summary, this study has utilized several new quantitative metrics for monitoring the kinetics of cell senescence, the number of cell cycles completed by WT cells versus mutants with accelerated telomere-shortening rates, and time-dependent changes that occur in both the morphological and physical properties of the cells. These results will facilitate future studies investigating genes and metabolic pathways that control cell aging as well as tests of environmental factors and chemicals that influence telomere shortening rates.

Acknowledgments

The authors wish to thank Victoria Lundblad for the generous gift of plasmid pVL715. This work was supported in part by National Institutes of Health grant 1R15AG028520-01A1.

References

[1]. Blackburn EH, Epel ES, Lin J, Human telomere biology: A contributory and interactive factor in aging, disease risks, and protection, Science 350 (2015) 1193–1198. [PubMed: 26785477]

[2]. McEachern MJ, Krauskopf A, Blackburn EH, Telomeres and their control, Annu. Rev. Genet 34 (2000) 331–358. [PubMed: 11092831]

[3]. Schmidt JC, Cech TR, Human telomerase: biogenesis, trafficking, recruitment, and activation, Genes Dev 29 (2015) 1095–1105. [PubMed: 26063571]

[4]. Shay JW, Role of Telomeres and Telomerase in Aging and Cancer, Cancer Discov 6 (2016) 584–593. [PubMed: 27029895]

[5]. Wu RA, Upton HE, Vogan JM, Collins K, Telomerase Mechanism of Telomere Synthesis, Annu. Rev. Biochem 86 (2017) 439–460. [PubMed: 28141967]

[6]. de Lange T, How telomeres solve the end-protection problem, Science 326 (2009) 948–952. [PubMed: 19965504]

[7]. Soudet J, Jolivet P, Teixeira MT, Elucidation of the DNA end-replication problem in Saccharomyces cerevisiae, Mol. Cell 53 (2014) 954–964. [PubMed: 24656131]

[8]. Cawthon RM, Smith KR, O'Brien E, Sivatchenko A, Kerber RA, Association between telomere length in blood and mortality in people aged 60 years or older, Lancet 361 (2003) 393–395. [PubMed: 12573379]

[9]. Arsenis NC, You T, Ogawa EF, Tinsley GM, Zuo L, Physical activity and telomere length: Impact of aging and potential mechanisms of action, Oncotarget 8 (2017) 45008–45019. [PubMed: 28410238]

[10]. Deng W, Cheung ST, Tsao SW, Wang XM, Tiwari AF, Telomerase activity and its association with psychological stress, mental disorders, lifestyle factors and interventions: A systematic review, Psychoneuroendocrinology 64 (2016) 150–163. [PubMed: 26677763]

[11]. Huzen J, Wong LS, van Veldhuisen DJ, Samani NJ, Zwinderman AH, Codd V, Cawthon RM, Benus GF, van der Horst JC, Navis G, Bakker SJ, Gansevoort RT, de Jong PE, Hillege HL, van Gilst WH, de Boer RA, van der Harst P, Telomere length loss due to smoking and metabolic traits, J. Intern. Med 275 (2014) 155–163. [PubMed: 24118582]

[12]. LaRocca TJ, Seals DR, Pierce GL, Leukocyte telomere length is preserved with aging in endurance exercise-trained adults and related to maximal aerobic capacity, Mech. Ageing Dev 131 (2010) 165–167. [PubMed: 20064545]

[13]. Paul L, Diet, nutrition and telomere length, J. Nutr. Biochem 22 (2011) 895–901. [PubMed: 21429730]

[14]. Shammas MA, Telomeres, lifestyle, cancer, and aging, Curr. Opin. Clin. Nutr. Metab. Care 14 (2011) 28–34. [PubMed: 21102320]

[15]. Ahmed W, Lingner J, Impact of oxidative stress on telomere biology, Differentiation 99 (2018) 21–27. [PubMed: 29274896]

[16]. Arndt GM, MacKenzie KL, New prospects for targeting telomerase beyond the telomere, Nat. Rev. Cancer 16 (2016) 508–524. [PubMed: 27339602]

[17]. Berardinelli F, Coluzzi E, Sgura A, Antoccia A, Targeting telomerase and telomeres to enhance ionizing radiation effects in in vitro and in vivo cancer models, Mutat. Res 773 (2017) 204–219. [PubMed: 28927529]

[18]. Jäger K, Walter M, Therapeutic Targeting of Telomerase, Genes (Basel), 7 (2016) 39.

[19]. Martínez P, Blasco MA, Telomere-driven diseases and telomere-targeting therapies, J. Cell Biol 216 (2017) 875–887. [PubMed: 28254828]

[20]. Campisi J, d'Adda di Fagagna F, Cellular senescence: when bad things happen to good cells, Nat. Rev. Mol. Cell Biol 8 (2007) 729–740. [PubMed: 17667954]

[21]. d'Adda di Fagagna F, Reaper PM, Clay-Farrace L, Fiegler H, Carr P, Von Zglinicki T, Saretzki G, Carter NP, Jackson SP, A DNA damage checkpoint response in telomere-initiated senescence, Nature 426 (2003) 194–198. [PubMed: 14608368]

[22]. Faragher RG, McArdle A, Willows A, Ostler EL, Senescence in the aging process, F1000Res 6 (2017) 1219. [PubMed: 28781767]

[23]. Hornsby PJ, Senescence and life span, Pflugers Arch 459 (2010) 291–299. [PubMed: 19763609]

[24]. Jeyapalan JC, Ferreira M, Sedivy JM, Herbig U, Accumulation of senescent cells in mitotic tissue of aging primates, Mech. Ageing Dev 128 (2007) 36–44. [PubMed: 17116315]

[25]. de Magalhães JP, Passos JF, Stress, cell senescence and organismal ageing, Mech. Ageing Dev 170 (2018) 2–9. [PubMed: 28688962]

[26]. Sedelnikova OA, Horikawa I, Zimonjic DB, Popescu NC, Bonner WM, Barrett JC, Senescing human cells and ageing mice accumulate DNA lesions with unrepairable double-strand breaks, Nat. Cell Biol 6 (2004) 168–170. [PubMed: 14755273]

[27]. Shen GP, Galick H, Inoue M, Wallace SS, Decline of nuclear and mitochondrial oxidative base excision repair activity in late passage human diploid fibroblasts, DNA Repair (Amst) 2 (2003) 673–693. [PubMed: 12767347]

[28]. Chen JH, Hales CN, Ozanne SE, DNA damage, cellular senescence and organismal ageing: causal or correlative? Nucleic Acids Res 35 (2007) 7417–7428. [PubMed: 17913751]

[29]. Derevyanko A, Whittemore K, Schneider RP, Jiménez V, Bosch F, Blasco MA, Gene therapy with the TRF1 telomere gene rescues decreased TRF1 levels with aging and prolongs mouse health span, Aging Cell 16 (2017) 1353–1368. [PubMed: 28944611]

[30]. Hwang ES, Yoon G, Kang HT, A comparative analysis of the cell biology of senescence and aging, Cell Mol. Life Sci 66 (2009) 2503–2524. [PubMed: 19421842]

[31]. Jaskelioff M, Muller FL, Paik JH, Thomas E, Jiang S, Adams AC, Sahin E, Kost-Alimova M, Protopopov A, Cadiñanos J, Horner JW, Maratos-Flier E, Depinho RA, Telomerase reactivation reverses tissue degeneration in aged telomerase-deficient mice, Nature 469 (2011) 102–106. [PubMed: 21113150]

[32]. Tomás-Loba A, Flores I, Fernández-Marcos PJ, Cayuela ML, Maraver A, Tejera A, Borrás C, Matheu A, Klatt P, Flores JM, Viña J, Serrano M, Blasco MA, Telomerase reverse transcriptase delays aging in cancer-resistant mice, Cell 135 (2008) 609–622. [PubMed: 19013273]

[33]. Xu M, Pirtskhalava T, Farr JN, Weigand BM, Palmer AK, Weivoda MM, Inman CL, Ogrodnik MB, Hachfeld CM, Fraser DG, Onken JL, Johnson KO, Verzosa GC, Langhi LGP, Weigl M, Giorgadze N, LeBrasseur NK, Miller JD, Jurk D, Singh RJ, Allison DB, Ejima K, Hubbard GB, Ikeno Y, Cubro H, Garovic VD, Hou X, Weroha SJ, Robbins PD, Niedernhofer LJ, Khosla S,

Tchkonia T, Kirkland JL, Senolytics improve physical function and increase lifespan in old age, Nat. Med 24 (2018) 1246–1256. [PubMed: 29988130]

[34]. Zhu Y, Tchkonia T, Pirtskhalava T, Gower AC, Ding H, Giorgadze N, Palmer AK, Ikeno Y, Hubbard GB, Lenburg M, O'Hara SP, LaRusso NF, Miller JD, Roos CM, Verzosa GC, LeBrasseur NK, Wren JD, Farr JN, Khosla S, Stout MB, McGowan SJ, Fuhrmann-Stroissnigg H, Gurkar AU, Zhao J, Colangelo D, Dorronsoro A, Ling YY, Barghouthy AS, Navarro DC, Sano T, Robbins PD, Niedernhofer LJ, Kirkland JL, The Achilles' heel of senescent cells: from transcriptome to senolytic drugs, Aging Cell 14 (2015) 644–658. [PubMed: 25754370]

[35]. Ballew BJ, Lundblad V, Multiple genetic pathways regulate replicative senescence in telomerase-deficient yeast, Aging Cell 12 (2013) 719–727. [PubMed: 23672410]

[36]. Khadaroo B, Teixeria MT, Luciano P, Eckert-Boulet N, Germann SM, Simon MN, Gallina I, Abdallah P, Gilson E, Géli V, Lisby M, The DNA damage response at eroded telomeres and tethering to the nuclear pore complex, Nat. Cell Biol 11 (2009) 980–987. [PubMed: 19597487]

[37]. Lundblad V, Blackburn EH, An alternative pathway for yeast telomere maintenance rescues est1-senescence, Cell 73 (1993) 347–360. [PubMed: 8477448]

[38]. Simon MN, Churikov D, Géli V, Replication stress as a source of telomere recombination during replicative senescence in Saccharomyces cerevisiae, FEMS Yeast Res 16 (2016) fow085 [PubMed: 27683094]

[39]. Teixeira MT, Saccharomyces cerevisiae as a Model to Study Replicative Senescence Triggered by Telomere Shortening, Front Oncol 3 (2013) 101. [PubMed: 23638436]

[40]. Wellinger RJ, Zakian VA, Everything you ever wanted to know about Saccharomyces cerevisiae telomeres: beginning to end, Genetics 191 (2012) 1073–1105. [PubMed: 22879408]

[41]. Lingner J, Hughes TR, Shevchenko A, Mann M, Lundblad V, Cech TR, Reverse transcriptase motifs in the catalytic subunit of telomerase, Science 276 (1997) 561–567. [PubMed: 9110970]

[42]. Becerra SC, Thambugala HT, Erickson AR, Lee CK, Lewis LK, Reversibility of replicative senescence in Saccharomyces cerevisiae: effect of homologous recombination and cell cycle checkpoints, DNA Repair (Amst) 11 (2012) 35–45. [PubMed: 22071150]

[43]. Enomoto S, Glowczewski L, Berman J, MEC3, MEC1, and DDC2 are essential components of a telomere checkpoint pathway required for cell cycle arrest during senescence in Saccharomyces cerevisiae, Mol. Biol. Cell 13 (2002) 2626–2638. [PubMed: 12181334]

[44]. Ijpma AS, Greider CW, Short telomeres induce a DNA damage response in Saccharomyces cerevisiae, Mol. Biol. Cell 14 (2003) 987–1001. [PubMed: 12631718]

[45]. Azam M, Lee JY, Abraham V, Chanoux R, Schoenly KA, Johnson FB, Evidence that the S. cerevisiae Sgs1 protein facilitates recombinational repair of telomeres during senescence, Nucleic Acids Res 34 (2006) 506–516. [PubMed: 16428246]

[46]. Claussin C, Chang MM, Multiple Rad52-Mediated Homology-Directed Repair Mechanisms Are Required to Prevent Telomere Attrition-Induced Senescence in Saccharomyces cerevisiae, PLoS Genet 12 (2016):e1006176. [PubMed: 27428329]

[47]. Brachmann CB, Davies A, Cost GJ, Caputo E, Li J, Hieter P, Boeke JD, Designer deletion strains derived from Saccharomyces cerevisiae S288C: a useful set of strains and plasmids for PCR-mediated gene disruption and other applications, Yeast 14 (1998) 115–132. [PubMed: 9483801]

[48]. Lewis LK, Lobachev K, Westmoreland JW, Karthikeyan G, Williamson KM, Jordan JJ, Resnick MA, Use of a restriction endonuclease cytotoxicity assay to identify inducible GAL1 promoter variants with reduced basal activity, Gene 363 (2005) 183–192. [PubMed: 16289630]

[49]. Nugent CI, Bosco G, Ross LO, Evans SK, Salinger AP, Moore JK, Haber JE, Lundblad V, Telomere maintenance is dependent on activities required for end repair of double-strand breaks, Curr. Biol 8 (1998) 657–660. [PubMed: 9635193]

[50]. Lewis LK, Westmoreland JW, Resnick MA, Repair of endonuclease-induced double-strand breaks in Saccharomyces cerevisiae: essential role for genes associated with nonhomologous end-joining, Genetics 152 (1999) 1513–1529. [PubMed: 10430580]

[51]. Sherman F, Getting started with yeast, Methods Enzymol 350 (2002) 3–41. [PubMed: 12073320]

[52]. Tripp JD, Lilley JL, Wood WN, Lewis LK, Enhancement of plasmid DNA transformation efficiencies in early stationary-phase yeast cell cultures, Yeast 30 (2013) 191–200. [PubMed: 23483586]

[53]. Joseph SB, Hall DW, Spontaneous mutations in diploid Saccharomyces cerevisiae: more beneficial than expected, Genetics 168 (2004) 1817–1825. [PubMed: 15611159]

[54]. Teng SC, Zakian VA, Telomere-telomere recombination is an efficient bypass pathway for telomere maintenance in Saccharomyces cerevisiae, Mol. Cell Biol 19 (1999) 8083–8093. [PubMed: 10567534]

[55]. Game JC, The Saccharomyces repair genes at the end of the century, Mutat. Res 451 (2000) 277–293. [PubMed: 10915878]

[56]. Kowalczykowski SC, An Overview of the Molecular Mechanisms of Recombinational DNA Repair, Cold Spring Harb. Perspect. Biol 7 (2015) a016410. [PubMed: 26525148]

[57]. San Filippo J, Sung P, Klein H, Mechanism of eukaryotic homologous recombination, Annu. Rev. Biochem 77 (2008) 229–257. [PubMed: 18275380]

[58]. Gao H, Toro TB, Paschini M, Braunstein-Ballew B, Cervantes RB, Lundblad V, Telomerase recruitment in Saccharomyces cerevisiae is not dependent on Tel1-mediated phosphorylation of Cdc13, Genetics 186 (2010) 1147–1159. [PubMed: 20837994]

[59]. Rizki A, Lundblad V, Defects in mismatch repair promote telomerase-independent proliferation, Nature 411 (2001) 713–716. [PubMed: 11395777]

[60]. Bärtsch S, Kang LE, Symington LS, RAD51 is required for the repair of plasmid double-stranded DNA gaps from either plasmid or chromosomal templates, Mol. Cell Biol 20 (2000) 1194–1205. [PubMed: 10648605]

[61]. Churikov D, Charifi F, Simon MN, Géli V, Rad59-facilitated acquisition of Y' elements by short telomeres delays the onset of senescence, PLoS Genet 10 (2014) e1004736. [PubMed: 25375789]

[62]. Game JC, Birrell GW, Brown JA, Shibata T, Baccari C, Chu AM, Williamson MS, Brown JM, Use of a genome-wide approach to identify new genes that control resistance of Saccharomyces cerevisiae to ionizing radiation, Radiat. Res 160 (2003) 14–24. [PubMed: 12816519]

[63]. Rao BS, Reddy NM, Genetic control of budding-cell resistance in the diploid yeast Saccharomyces cerevisiae exposed to gamma-radiation, Mutat. Res 95 (1982) 213–224. [PubMed: 6750384]

[64]. Saeki T, Machida I, Nakai S, Genetic control of diploid recovery after gamma-irradiation in the yeast Saccharomyces cerevisiae, Mutat. Res 73 (1980) 251–265. [PubMed: 7007877]

[65]. Symington LS, Role of RAD52 epistasis group genes in homologous recombination and double-strand break repair, Microbiol. Mol. Biol. Rev 66 (2002) 630–670. [PubMed: 12456786]

[66]. Le S, Moore JK, Haber JE, Greider CW, RAD50 and RAD51 define two pathways that collaborate to maintain telomeres in the absence of telomerase, Genetics, 152 (1999) 143–152. [PubMed: 10224249]

[67]. Maringele L, Lydall D, Telomerase- and recombination-independent immortalization of budding yeast, Genes Dev 18 (2004) 2663–2675. [PubMed: 15489288]

[68]. Chang HY, Lawless C, Addinall SG, Oexle S, Taschuk M, Wipat A, Wilkinson DJ, Lydall D, Genome-wide analysis to identify pathways affecting telomere-initiated senescence in budding yeast, G3 (Bethesda) 1 (2011) 197–208. [PubMed: 22384331]

[69]. Matsui A, Matsuura A, Cell size regulation during telomere-directed senescence in Saccharomyces cerevisiae, Biosci. Biotechnol. Biochem 74 (2010) 195–198. [PubMed: 20057141]

[70]. Mourant JR, Freyer JP, Hielscher AH, Eick AA, Shen D, Johnson TM, Mechanisms of light scattering from biological cells relevant to noninvasive optical-tissue diagnostics, Appl. Optics 37 (1998) 3586–3593.

[71]. Münch T, Sonnleitner B, Fiechter A, The decisive role of the Saccharomyces cerevisiae cell cycle behaviour for dynamic growth characterization, J. Biotechnol 22 (1992) 329–351. [PubMed: 1367988]

[72]. Porro D, Srienc F, Tracking of individual cell cohorts in asynchronous Saccharomyces cerevisiae populations, Biotechnol. Prog 11 (1995) 342–337. [PubMed: 7619403]

[73]. Neurohr GE, Terry RL, Lengefeld J, Bonney M, Brittingham GP, Moretto F, Miettinen TP, Vaites LP, Soares LM, Paulo JA, Harper JW, Buratowski S, Manalis S, van Werven FJ, Holt LJ, Amon A, Excessive cell growth causes cytoplasm dilution and contributes to senescence, Cell 176 (2019) 1083–1097. [PubMed: 30739799]

Highlights (Ghanem et al.)

New techniques allowed quantitative analysis of senescence in the yeast model system
Loss of recombination genes RAD51, RAD52 or RAD54 strongly accelerated senescence
Senescence was only modestly affected by inactivation of RAD55, RAD57 or RAD59
High resolution microscopy revealed 60% increases in cells' sizes during senescence
New assays revealed time-dependent changes in physical properties of senescent cells

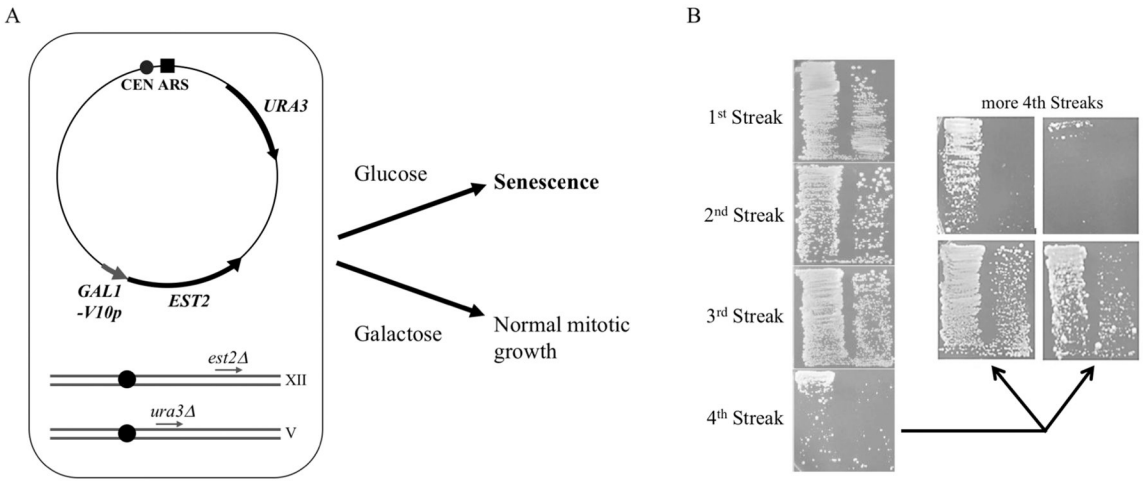

Fig. 1.

Method employed to monitor senescence in the yeast model system. (A) Strain YLKL803 contains the plasmid pLKL82Y, which expresses *EST2* from a mutant *GAL1* promoter that has reduced basal activity. (B) Example of a traditional senescence streak assay revealing the reduced but variable growth observed on the last streak.

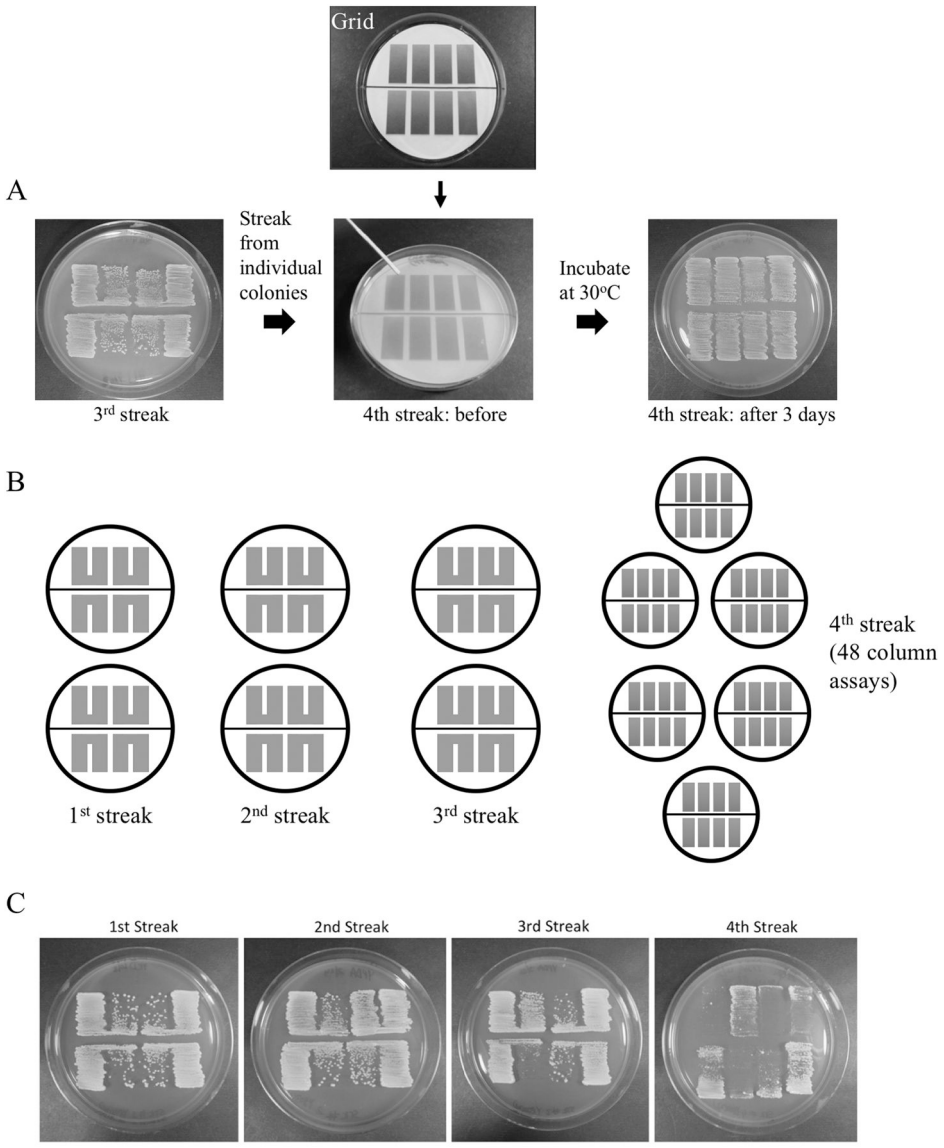

Fig. 2.

Illustration of new method for quantitative analysis of senescence rates. (A) Cells are streaked repeatedly from single colonies to form new isolated colonies in the traditional manner for the first three streak plates. For the final senescence plate, colonies are streaked into single rectangular columns using a grid has been placed under the plate. In the example shown, YLKL803 (*GAL1-V10::EST2*) was grown on galactose plates, making the cells $Est2^{+}$, which resulted in 8 full columns of growth on the 4th streak. (B) A key element of this approach is that colonies are picked and streaked to new plates multiple times (two plates for each strain with four double columns per plate). This procedure generates many colonies that are individually streaked into 48 single columns on the 4th streak plate, in essence creating 48 separate senescence tests. (C) Examples of senescence assay plates 1, 2, 3 and 4 resulting from repeatedly streaking YLKL803 cells to YPDA plates. In this typical example, several incomplete columns are observed on the 4th streak plate.

A

est2 cell senescence: YPDA vs synthetic media

	Gal-Ura	YPDA (4th streak)			Glu-complete (4th streak)		
		Trial 1	Trial 2	Trial 3	Trial 1	Trial 2	Trial 3
Full columns	46/48	7/32	12/48	11/48	13/32	18/48	21/48
Avg/plate (#/8 ± SD)	7.7 ± 0.5	1.8 ± 1.7	2.0 ± 1.1	1.8 ± 1.7	3.3 ± 2.1	3.0 ± 1.3	3.5 ± 1.9
Median	8.0	1.5	2.0	2	3.5	3.5	4.0

B

est2 cells: 3rd streak

	3rd streak (*est2*)	
	Trial 1	Trial 2
Full columns	42/48	47/48
Avg/plate (#/8 ± SD)	7.0 ± 1.5	7.8 ± 0.4
Median	7.0	8.0

C

est2 rad52 cells: 3rd streak

	3rd streak (*est2 rad52*)	
	Trial 1	Trial 2
Full columns	6/48	7/48
Avg/plate (#/8 ± SD)	1.0 ± 1.3	1.2 ± 1.3
Median	0.5	1.0

D

Senescence of *est2* cells deficient in production of homologous recombination proteins

	3rd streak						
	est2	*rad51 est2*	*rad52 est2*	*rad54 est2*	*rad55 est2*	*rad57 est2*	*rad59 est2*
Full columns	45/48	7/48	4/48	6/48	44/96	27/80	23/48
Avg/plate (#/8±SD)	7.5 ± 0.6	**1.2** ± 1.8	**0.7** ± 1.2	**1.0** ± 1.1	3.7 ± 1.9	2.7 ± 2.2	3.8 ± 2.6
Median	7.5	0.0	0.0	1.0	3.5	2.5	4.0
Student's T-test		p = 0.00	p = 0.00	p = 0.00	p = 0.00	p = 0.00	p = 0.03

E

est2 cell senescence: alternative assay strain

	4th streak – (pVL715) Glu-complete
Full columns	20/48
Avg/plate (#/8 ± SD)	3.3 ± 1.5
Median	3.0

Fig. 3.

Quantitation of senescence in *est2* and *est2 rad52* cells using the column assay method. (A) Results obtained from analysis of 4th streak plates. Senescence assays were performed using YLKL803 cells propagated on either YPDA or synthetic complete glucose plates. Results from three separate assays (trials) conducted weeks apart are shown. (B and C) Results of assays performed by streaking cells from individual colonies into single columns on the 3rd streak rather than on the 4th streak using YPDA plates. As expected, most *est2* cells formed full columns on the 3rd streak plate, but *est2 rad52* cells did not. (D) Plate senescence assays demonstrating the consequences of inactivating several RAD52 epistasis group genes involved in homologous recombination. (E) A different senescence assay strain (YLKL961) containing pVL715 (*ADH1p::EST2 URA3*) produces results similar to YLKL803 (*GAL1-V10::EST2*). Cells were streaked to synthetic glucose plates containing 5-FOA initially to

select for cells that had lost the plasmid, followed by repeated streaking of the plasmidless cells to glucose complete plates.

A

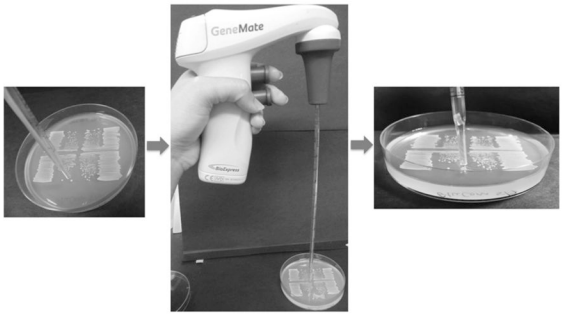

B

Calculation of population doublings

Cell cycles completed beginning from one cell	Number of cells in each colony
1st generation	2
2nd generation	4
.	.
.	.
18th generation	262,144
19th generation	524,288
20th generation	1,048,576

C

est2 cells grown on YPDA media

YPDA plates	Cells per colony	No. generations (± SD)
Streak 1	$3.4x10^6$	21.6 ± 0.3
Streak 2	$4.4x10^6$	22.0 ± 0.4
Streak 3	$2.4x10^6$	21.1 ± 0.3
Total		64.7

D

est2 cells grown on synthetic media

Synthetic glucose plates	Cells per colony	No. generations (± SD)
Streak 1	$3.0x10^6$	21.4 ± 0.4
Streak 2	$3.4x10^6$	21.6 ± 0.3
Streak 3	$1.4x10^6$	20.3 ± 0.4
Total		63.3

E

est2 rad52 cells grown on YPDA media

YPDA plates	Cells per colony	No. generations (± SD)
Streak 1	$3.9x10^6$	21.8 ± 0.6
Streak 2	$1.5x10^6$	20.5 ± 0.8
Total		42.3

F

est2 rad52 cells grown on synthetic media

Synthetic glucose plates	Cells per colony	No. generations (± SD)
Streak 1	$3.0x10^6$	21.4 ± 0.3
Streak 2	$2.8x10^6$	21.3 ± 0.2
Total		42.7

Fig. 4.

Determination of the number of population doublings (generations of growth) achieved by telomerase-deficient cells during senescence. (A) Photo array depicting the use of a long 1 mL pipette and pipette controller to core individual colonies from senescence assay plates. (B) Relationship between generations of growth from a single cell and total numbers of cells within the resulting colonies. (C and D) Average cells per colony and cell cycles completed for *est2* cells grown on YPDA or synthetic complete glucose plates. (E and F) Cells per colony and cell cycles completed were determined for *est2 rad52* cells.

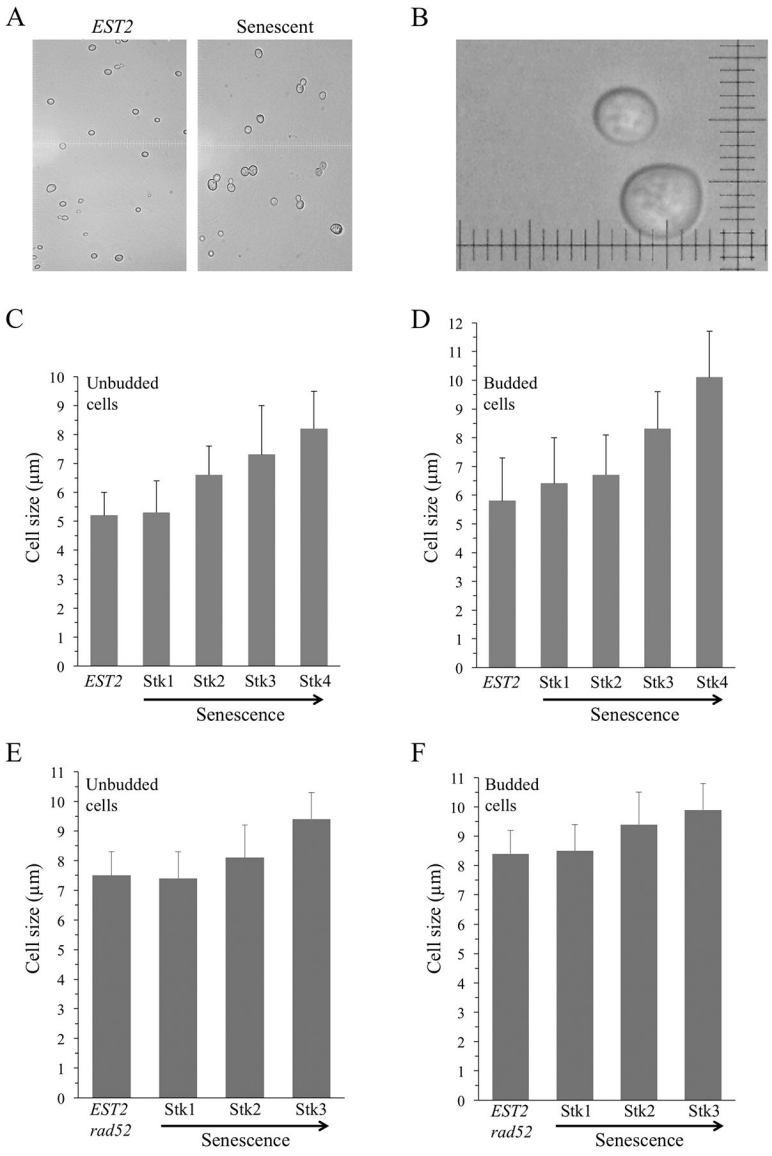

Fig. 5.

Cell size increases progressively during senescence. (A) Phase contrast images of wildtype and senescent (4th streak plate) cells. (B) Example of method used to measure the maximum diameters of cells. (C and D) Average sizes of unbudded and budded cells assessed at different stages of senescence. (E and F) Average sizes of unbudded and budded *est2 rad52* cells. WT, telomerase-proficient BY4742 cells. Stk1, Stk2, Stk3 and Stk4 refer to the 1st, 2nd, 3rd and 4th streak plates. Error bars indicate standard deviations.

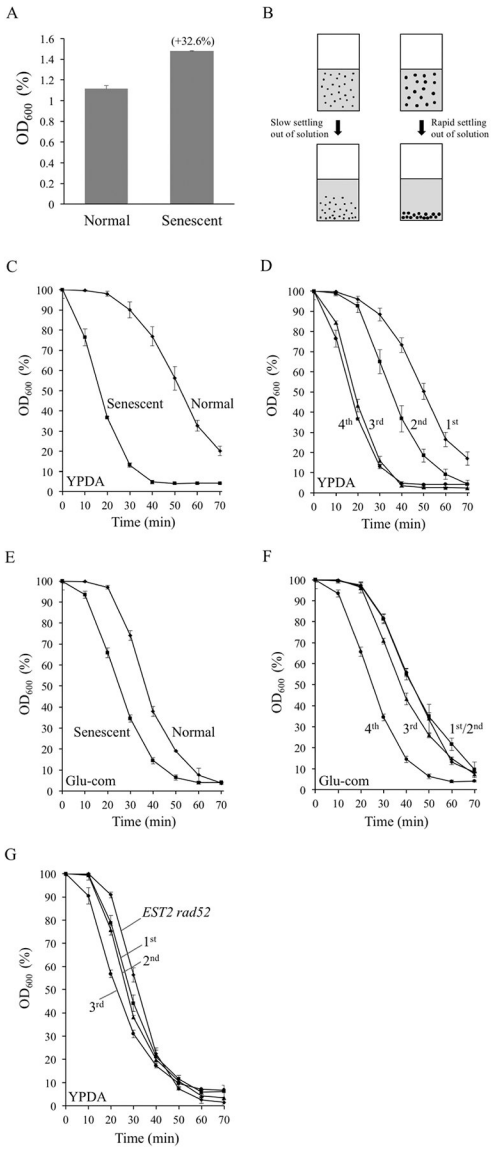

Fig. 6.

Assessment of time-dependent changes in the physical properties of cells during senescence. (A) Light scattering at 600 nm is increased in senescent cells. Wildtype and senescent (4^{th} streak plate) cells were sonicated and set to a titer of 1×10^7 cells per mL. Five replicates of each strain were analyzed. (B) Diagram illustrating the concept underlying cell sedimentation rate studies, i.e., larger cells tend to fall faster than smaller cells and the process can be monitored as a reduction in OD_{600} over time. (C) Time course of cell sedimentation in wildtype vs. fully senescent cells propagated on rich YPDA plates. (D) Progressive changes in sedimentation rates harvested from 1^{st}, 2^{nd}, 3^{rd} and 4^{th} streak YPDA plates. (E) Sedimentation of wildtype and fully senescent cells grown on synthetic glucose plates. (F) Sedimentation results for cells harvested from 1^{st}, 2^{nd}, 3^{rd} and 4^{th} streak synthetic glucose plates. (G) Time course of sedimentation of non-senescent *rad52* cells (*EST2 rad52*)

and for 1st, 2nd and 3rd streak plates containing *est2 rad52* cells. Error bars indicate standard deviations. Glu-com, synthetic glucose complete media.